Chemical, electrical and electrochemical characterization of hybrid organic/inorganic polypyrrole/$PW_{12}O_{40}{}^{3-}$ coating deposited on polyester fabrics

J. Molina, J. Fernández, A.I. del Río, J. Bonastre, F. Cases [*]

Departamento de Ingeniería Textil y Papelera, EPS de Alcoy, Universitat Politècnica

de València, Plaza Ferrándiz y Carbonell s/n, 03801 Alcoy, Spain

Abstract

A study of the stability of conducting fabrics of polyester (PES) coated with polypyrrole/$PW_{12}O_{40}{}^{3-}$ (organic/inorganic hybrid material) in different pH solutions (1, 7, 13) has been done. Washing tests were also done in views of its possible application in electronic textiles such as antistatic clothing. X-ray photoelectron spectroscopy (XPS) studies have been done to quantify the amount of counter ion that remains in the polymer matrix and determine the doping ratio (N^+/N) after the different tests. Scanning electron microscopy (SEM) was also used to observe morphological differences after the different tests. Surface resistivity changes were measured by means of electrochemical impedance spectroscopy (EIS). Scanning electrochemical microscopy (SECM) was employed to measure changes in electroactivity after the different tests. Higher pHs caused a decrease of the doping ratio (N^+/N), the loss of part of the counter ions and the decrease of its conducting and electrocatalytic properties. The stability in acid, neutral media and after the washing test was good. Only at pH 13 the loss of the counter ion was widespread and there was a decrease of its conducting and catalytic properties; although the fabrics continued acting mainly as a conducting material.

1

———————————————

* Corresponding author. Tel.: +34 966528412; Fax.: +34 96 652 8438

E-mail address: fjcases@txp.upv.es (Prof. F. Cases)

1. Introduction

The development of textiles with new properties and applications has received great attention during the last years; one of these properties is the electrical conductivity. One of the methods that have been employed to produce conducting fabrics is the chemical synthesis of polypyrrole on fabrics [1-9]. Applications of polypyrrole-based conducting fabrics are varied and numerous; like antistatic materials [1], gas sensors [2], biomechanical sensors [3], electrotherapy [4, 5], heating devices [6-8] or microwave attenuation [9].

During the formation of polypyrrole, positive charges are created in its structure (polarons and bipolarons). These positive charges are compensated by anions that act as counter ions to maintain the electroneutrality principle. Low size anions such as Cl^- have been employed as counter ions, but their stability is low [9]. If the counter ion is expelled from the structure (dedoping), there is a great loss of its electrical properties. To prevent this phenomenon, bulky anions with a high molecular size have been employed in bibliography. When the size of the counter ion is high, its diffusion is prevented and it remains in the polypyrrole structure [10]. The higher size of the counter ion, the more difficult the expulsion of the counter ion from the structure is. Typical

counter ions employed in textiles coated with polypyrrole, are organic molecules with high size; like anthraquinone sulfonic acid (AQSA) [2, 7, 9, 11-14], dodecylbenzene sulfonic acid (DBSA) [1, 12], p-toluene sulfonic acid (PTSA) [2, 9, 12, 15], naphthalenedisulfonic acid (NDSA) [3, 9, 12], benzenesulfonic acid (BSA) [4, 16], naphthalenesulfonic acid (NSA) [9, 15], anthraquinone disulfonic acid [17, 18].

However, very little has been reported about the use of inorganic anions as counter ions when obtaining conducting fabrics. In our previous work [14], we employed an inorganic anion as counter ion ($PW_{12}O_{40}^{3-}$) to produce polypyrrole-based conducting fabrics. A hybrid organic/inorganic layer was obtained ($PPy/PW_{12}O_{40}^{3-}$). $PW_{12}O_{40}^{3-}$ is a polyoxometalate (POM) with high volume and charge [19], so their diffusion coefficient is low, and the exchange with anions present in the solution is prevented. In addition to this, $PW_{12}O_{40}^{3-}$ presents also catalytic properties [20, 21].

One of the applications that our group aims to is the employment of conducting fabrics in catalysis, or as a support with high surface area to electrodeposit Pt nanoparticles and enhance its electroactivity [22, 23]. For example, conducting polymers have been employed in environmental applications; electrodes modified with conducting polymers have been used in Cr^{6+} (toxic) reduction to Cr^{3+} (not toxic) [24] or nitrites electroreduction [25]. The employment of polypyrrole coated textiles in the electrochemical removal of the textile dye C. I. Direct Red 80 has been also reported [26]. Polyaniline/MnO_2 catalyst and H_2O_2 as an oxidant have been employed in the degradation of organic dyes such as Direct Red 81, Indigo Carmine and Acid Blue 92 [27, 28]. For these purposes, the study of the stability of the $PPy/PW_{12}O_{40}^{3-}$ layer and its properties in different pH solutions is essential to optimize its operational pH range.

Another application that we are studying at present is its employment in electronic clothing, for instance its antistatic or microwave attenuation properties. For this purpose, the conducting fabrics would have to resist washing tests. X-ray photoelectron spectroscopy (XPS) measurements have been used to quantify the amount of counter ion ($PW_{12}O_{40}^{3-}$) present in the polypyrrole matrix and the doping ratio (N^+/N) after the different tests. Scanning electron microscopy (SEM) and energy dispersive X-ray (EDX) measurements have been employed for morphology observation and zonal analysis, respectively. Surface resistivity ($\Omega/\square$) changes have been measured by electrochemical impedance spectroscopy (EIS) after the different tests. The electroactivity of the samples after the different tests has been measured by scanning electrochemical microscopy (SECM). SECM is a relatively novel (1989) and powerful technique that is becoming more popular among researchers [29-31]. Its employment in conducting fabrics has not been reported since the most employed substrate in bibliography is Pt.

2. Experimental

2.1. Reagents and materials

Analytical grade pyrrole, ferric chloride, sulphuric acid, sodium dihydrogenophosphate, disodium hydrogenophosphate, sodium sulfate and sodium hydroxide were purchased from Merck. Normapur acetone was from Prolabo. Analytical grade phosphotungstic acid hydrate was supplied by Fluka. Ultrapure water was obtained from an Elix 3 Millipore-Milli-Q Advantage A10 system with a resistivity near to 18.2 MΩ cm. Polyester textile was acquired from Viatex S.A. and their characteristics were: fabric

surface density, 140 g m^{-2}; warp threads per cm, 20 (warp linear density, 167 dtex); weft threads per cm, 60 (weft linear density, 500 dtex). These are specific terms used in the field of textile industry and their meaning can be consulted in a textile glossary [32].

2.2. Chemical synthesis of PPy/PW$_{12}$O$_{40}$$^{3-}$ on polyester fabrics

Chemical synthesis of PPy on polyester textiles was done as reported in our previous study [14]. The size of the samples was 6 cm x 6 cm approximately. Previously to reaction, polyester was degreased with acetone in ultrasound bath and washed with water. Pyrrole concentration employed was 2 g l^{-1} and the molar relations of reagents employed in the chemical synthesis bath were pyrrole: FeCl$_3$: H$_3$PW$_{12}$O$_{40}$ (1: 2.5: 0.2). The next stage was the adsorption of pyrrole and counter ion (PW$_{12}$O$_{40}$$^{3-}$) (V=200 ml) on the fabric for 30 min in an ice bath without stirring. At the end of this time, the FeCl$_3$ solution (V=50 ml) was added and oxidation of the monomer took place during 150 min without stirring. Adsorption and reaction were performed in a precipitation beaker. The conducting fabric was washed with water to remove PPy not joined to fibers and dried in a desiccator for at least 24 h before measurements. The weight increase obtained was around 10 %. The thickness of the film obtained on the fibers of the fabric was around 600 nm.

2.3. Stability of PW$_{12}$O$_{40}$$^{3-}$ in the conducting textiles of PES-PPy/PW$_{12}$O$_{40}$$^{3-}$ in different pH solutions

Different samples of PES-PPy/PW$_{12}$O$_{40}$$^{3-}$ (2 cm x 2 cm) were soaked in different pH solutions. The solutions employed were: 0.1 M H$_2$SO$_4$ (pH~1), phosphates buffer + 0.1 M Na$_2$SO$_4$ (pH~7) and 0.1 M NaOH + 0.1 M Na$_2$SO$_4$ (pH~13). After 1 h of contact

with the different pH solutions, the samples were rinsed with ultrapure water and dried in a desiccator before measurements. Different samples were obtained equally to perform the different analysis. XPS analyses were done to quantify the amount of counter ion and doping ratio (N^+/N). Zonal analyses were performed by means of EDX and morphological changes in the coating were also observed by means of SEM. Surface resistivity and electroactivity changes were measured by EIS and SECM, respectively.

2.4. Washing tests

Washing tests were performed to test the stability of the coating and its properties after these tests. The analysis was done as related in the norm ISO 105-C01 at 40º C during 30 min. The different analysis mentioned in section 2.3. were also done for these samples.

2.5. X-ray photoelectron spectroscopy measurements

XPS analyses were conducted at a base pressure of at $5 \cdot 10^{-10}$ mbars and a temperature around 173 K. The XPS spectra were obtained with a VG-Microtech Multilab electron spectrometer by using unmonochromatized Mg Kα (1253.6 eV) radiation from a twin anode source operating at 300 W (20 mA, 15 KV). The binding energy (BE) scale was calibrated with reference to the C1s line at 284.6 eV. The C1s, O1s, N1s, S2p, P2p and W4f core levels spectra were analyzed for the original sample of PES-PPy/$PW_{12}O_{40}^{3-}$, and samples of PES-PPy/$PW_{12}O_{40}^{3-}$ after contact with different pH solutions (1, 7, 13) and after the washing test.

2.6. SEM and EDX characterization

A Jeol JSM-6300 scanning electron microscope was employed to observe the morphology of the samples and perform EDX analyses. SEM micrographs were obtained using an acceleration voltage of 20 kV. EDX measurements were done between 0 and 20 keV.

2.7. Electrochemical impedance spectroscopy measurements

An Autolab PGSTAT302 potentiostat/galvanostat was employed to perform electrochemical impedance spectroscopy (EIS) analyses. EIS measurements were performed in the 10^5-10^{-2} Hz frequency range. The amplitude of the sinusoidal voltage employed was $\pm$ 10 mV. Measurements were carried out using two rectangular copper electrodes (0.5 cm x 1.5 cm) separated by 1.5 cm and pressed to the dry textile sample. The measured area of the textile was a square of 1.5 cm, so when the material acts as a resistor, the measured impedance modulus (Ω) was equal to the surface resistivity ($\Omega/\square$).

2.8. Scanning electrochemical microscopy measurements

SECM measurements were carried out with a scanning electrochemical microscope of Sensolytics. The three-electrode cell configuration consisted of a 100-μm-diameter Pt ultra-microelectrode (UME) working electrode, a Pt wire auxiliary electrode and an Ag/AgCl (3 M KCl) reference electrode. The solution selected for this study was 0.01 M $Ru(NH_3)_6Cl_3$ in aqueous 0.1 M KCl supporting electrolyte. All the experiments were carried out in inert nitrogen atmosphere. Substrates of PES and the samples of PES-$PPy/PW_{12}O_{40}{}^{3-}$ after the different pH treatments were chosen as substrates for the

SECM measurements. The different samples were glued with epoxy resin on glass microscope slides.

The positioning of the Pt UME tip was achieved by first carefully putting it in contact with the substrate surface and then moving it in z direction (height of the electrode). Once the electrode was at the desired height, the electrode was approached to the substrate surface; the current of the UME was recorded to obtain the approach curves. Approach curves give us an indication of the electroactivity of the surface.

3. Results and discussion

3.1. XPS analysis of PES-PPy/$PW_{12}O_{40}^{3-}$ treated at different pHs

XPS analyses were done to quantify the amount of counter ion ($PW_{12}O_{40}^{3-}$) and doping ratio (N^+/N) of the fabrics after the different tests. The C1s, O1s, N1s, S2p, P2p and W4f core levels spectra were analyzed for the different PES-PPy/$PW_{12}O_{40}^{3-}$ samples. Table 1 shows chemical composition and doping ratio (N^+/N) for polypyrrole/$PW_{12}O_{40}^{3-}$ (PPy/POM) coated textiles. Samples 2 to 4 were previously treated with different solutions. These hybrid materials should ideally have the formula $C_4H_3N(PW_{12}O_{40}^{3-})_x$, where "x" is the fractional doping level obtained by W analysis. XPS analyses showed a systematic carbon excess, which may be due to surface hydrocarbon contamination [33]. The composition analyses showed also an oxygen excess in all specimens. This may be due to PPy ring oxidation attributed to PPy reaction with water as synthesis solvent [34]. POM fractional doping level suffered a gradual decrease when samples were treated in more basic solutions. Sample 4 showed a complete counter ion lose due to the disintegration of $PW_{12}O_{40}^{3-}$. These facts will be explained in detail later.

3.1.1. C1s analysis

Fig. 1 shows the deconvoluted high resolution C1s spectrum for an untreated specimen (sample 1). Three peaks appear at the following binding energies: 284.3, 285.8 and 287.8 eV. The contribution at the lowest binding energy was due to C-C/C-H groups [35]. The peak at 285.8 eV was assigned to C-N groups in the pyrrole rings [35-37]. The binding energy peak at 287.8 eV was ascribed to carbonyl C=O groups [38, 39]. The appearance of C=O groups was mainly due to the presence of pyrrole overoxidation during chemical polymerization in aqueous media, as commented before. It has been proved that polypyrrole is simultaneously degraded during the synthesis in short soluble maleimide molecules. This degradation process may be attributed to the polymer overoxidation which is described as a gradual polymer oxidation by water in the presence of $FeCl_3$. Quantitative measurements confirmed that polymerization presented second-order kinetics with regard to $FeCl_3$, while overoxidation appeared to be only first order [32]. Contamination with particulated PPy might also appear on the surface due to the formation of aggregates and individual particles of colloidal PPy [40]. Fig. 1 shows that C-C/C-H peak area is significantly greater than the C-N one. For the pyrrole structure, the atomic ratio (C-C/C-H)/C-N must be equal to 1.0. The higher C-C/C-H contribution is coherent with a maleimide-like structure where C=O groups appear at α positions (C-N groups). This overoxidation might be estimated as the atomic ratio $C=O/C_{Total}$, obtaining a value around 10 % for the original PES-PPy/$PW_{12}O_{40}^{3-}$ sample. As surface hydrocarbon contamination may be present, this is a minimum value. Important changes in overoxidation state were not appreciated as a result of treating the PPy/POM samples in different pH solutions (values between 10-13 % were obtained).

Table 2 shows the C1s, O1s, N1s, S2p, P2p and W4f core level binding energies assignments for PPy/POM untreated and treated with pH 1, 7 and 13 solutions. Noticing in C1s binding energies, there were not important changes in the binding energies obtained for the different specimens. The same chemical carbon groups, commented previously, appeared for the four samples.

3.1.2. O1s analysis

Fig. 2 shows the high resolution O1s spectrum for the untreated specimen (sample 1). The O1s core level peak was deconvoluted in two contributions centered at 530.5 and 532.0 eV. These contributions were attributed, respectively, to W-O-W groups and W=O groups in the $PW_{12}O_{40}^{3-}$ counter ion [41]. Seeing Table 2, the binding energy results for sample 1, 2 and 3 are very similar. Therefore, the same contributions can be expected for samples 1 to 3 since $PW_{12}O_{40}^{3-}$ is present in the chemical composition of the different samples (Table 1).

The analysis performed for sample 4 shows that the O1s spectrum exhibited three peaks in the sites 530.5, 532.0 and 533.6 eV. On one hand, the peak at 530.5 eV was caused by C=O group. The peak at 532.0 eV was due to SO_4^{2-} and is due to incorporated counter ion within the polymer [42]. The S2p analysis also showed the presence of two peaks due to SO_4^{2-} (section 3.1.6.) and corroborates the SO_4^{2-} presence. As a high pH (pH 13) is used for the treatment with $Na_2SO_4 + NaOH$ solution, the counter ion will be predominantly in the sulfate rather than bisulfate form. The peak at 533.6 eV has been attributed to C=O-C groups [35].

In samples 1, 2 and 3, the contributions that for C=O, C=O-C, SO_4^{2-} did not appear, probably due to a high oxygen content from POM molecules, 40 oxygen atoms per $PW_{12}O_{40}^{3-}$ molecule ($PW_{12}O_{40}^{3-}$). In sample 4, the oxygen content from POM counter

ion did not interfere because this counter ion had been almost completely released from the polymer matrix (Table 1).

3.1.3. N1s analysis

Fig. 3 shows the high resolution N1s spectrum for the untreated specimen (sample 1). The N1s spectrum was deconvoluted into two contributions, centered at 399.9 and 401.5 eV. The peak at 399.9 eV was assigned to the neutral amine-like (–NH–) structure which is characteristic of pyrrolylium nitrogen [35, 38, 43]. The peak at 401.5 eV was attributed to positively charged nitrogen, N^+. The electron-deficient nitrogen species arise from delocalization of electron density from the polypyrrole ring as a result of the formation of electronic defects (polarons and bipolarons) [36, 43]. The doping ratio represented by the (N^+/N) ratio was found to be 0.23. As POM presents 3 negative charges per molecule, the POM fractional doping level obtained by N analysis would be $0.23/3 = 0.076$, value lower than the value of 0.115 obtained by W analysis. This indicates an incorporation of the counter ion in excess; probably caused by the presence of aggregates of polypyrrole on the surface of the fabric.

The same nitrogen functional groups appeared when samples were treated in pH 1 and 7 solutions. As commented before, these peaks were due to neutral amine-like (–NH–) structure and positively charged nitrogen, N^+. The doping ratios obtained for the samples treated in pH 1 and pH 7 solutions were 0.20 and 0.27, respectively. These variations of the doping ratio were not significative and they could be attributed to zonal variations within the fabric. On the other hand, the N1s spectrum of the sample treated at pH 13 presented significant changes; two peaks were observed at 398.0 and 400.0 eV. The peak at 400.0 eV was assigned to neutral amine-like (–NH–) structure. The

contribution at 398.0 eV has been attributed to deprotonated and uncharged imine-like nitrogens (>C=N-) [38, 44]. The N^+ contribution disappeared completely from the N1s spectrum (compare figure 3 and 4). This fact also confirmed the loss of POM anions, undergoing decomposition (as it will be explained in the W4f analysis). For the samples 2-4 (treated in media containing sulfates) the appearance of sulfur in the XPS spectrum (figure not shown) confirmed also the incorporation of sulfates in the polymer matrix. The sulfates content can be observed in table 1.

3.1.4. P2p analysis

Phosphorous was also detected despite the small quantity within the counter ion (1 atom of P per 12 of W). P2p analyses showed the presence of a band to P at 133.7 eV (figure not shown). This band has been observed in other studies of polyoxometalates [45-48]. The quantification of counter ion taking into account the amount of P was not reliable given the small amount of P. In addition, the atom of P is also in the center of the polyoxometalate and only part of the photoelectrons can be detected [45]. Therefore, the quantification of the counter ion was done according to W analyses.

3.1.5. W4f analysis

Fig. 5 shows the high resolution W4f spectrum for untreated PPy/POM sample. A spin-orbit coupling doublet appeared at 35.4 eV ($W4f_{7/2}$) and 37.5 eV ($W4f_{5/2}$). This doublet is due to W^{6+} that comes from the counter ion, $PW_{12}O_{40}^{3-}$ [46, 49]. In addition, this doublet with a separation of 2.1 eV is also characteristic of W^{6+} oxidation state [50]. The same binding energies were obtained for samples 2 and 3. The content of the counter ion (Table 1) decreased gradually with the pH from 0.115 of the original sample

to: 0.057 (pH 1), 0.040 (pH 7). When the sample was immersed for 1 hour in pH 13 solution, there was a great decrease of the POM content (0.0003) although the two peaks at 35.2 and 37.3 eV arising from W^{6+} were still detected. The presence of W was minimal in the polymer coating; NaOH treatment had caused the removal of the dopant, $PW_{12}O_{40}{}^{3-}$. This fact is coherent with data obtained for N1s analysis that shows the disappearance of the N^+ peak. Zu et al. corroborated that the $PW_{12}O_{40}{}^{3-}$ molecule suffers decomposition into $PO_4{}^{3-}$ and $WO_4{}^{2-}$ at pH>8.3 [51], so the treatment at pH 13 caused the total decomposition of the POM dopant and its removal from the polymer matrix.

3.1.6. S2p analysis

The treatment of conducting fabrics with the different pH solutions caused the removal of part of the $PW_{12}O_{40}{}^{3-}$ counter ions. Therefore, sulfate anions could be incorporated as counter ions and replace them. This fact can be observed in Table 1. S2p measurements showed the presence of two bands at 168.2 and 169.6 eV (Table 2). This doublet is attributed to S2p1/2 and S2p3/2 of sulfates [52].

3.2. Washing test of the conducting textile

Sample 1 was submitted to washing test as related in the norm ISO 105-C01. It is important to know the conductivity of the conducting fabric after laundering tests in views of employing them in electronic textiles. In that sense, Hurren et al. studied the influence of the detergent and washing temperature on the conductivity of conducting fabrics of polypyrrole/AQSA [53]. This sort of studies has been done in the case of using organic counter ions [53, 54]. The effect of laundering in the case of employing inorganic counter ions has not been reported. In addition to conductivity changes, it is

also important to know the doping ratio (N^+/N) and the fractional doping level (counter ion content) after washing tests. If the conducting textile suffers a complete dedoping (release of the counter ion), this textile loses its conducting properties. XPS analysis allows the quantification of the counter ion that remains in the polymer structure, as well as the doping ratio determination. The chemical composition obtained by XPS analysis was: $C_{9.92}N(PW_{12}O_{40}^{3-})_{0.054}O_{1.47}$. The amount of dopant decreased from 0.115 for the original sample (Table 1) to 0.054 after washing, so the quantity of dopant remaining in the coating was around 47 %. This value is high enough taking into account the aggressive test of washing. The doping ratio obtained was not substantially modified (0.20) regardless the partial loss of counter ion observed. On the other hand, the oxygen excess content increased from 0.32 to 1.47 after washing.

3.3. SEM and EDX measurements

EDX analysis can be used as a semi-quantitative analysis to measure the W content in the conducting fabrics after the different tests. In Fig. 6-a it can be observed the EDX analysis of the sample of PES-PPy/$PW_{12}O_{40}^{3-}$ in the area of the micrograph attached. As can be seen, different W bands are observed. The presence of Fe is due to the use of $FeCl_3$ as oxidant during the synthesis of the polymer. The morphology of the layer of polypyrrole can also be observed in the micrograph. It can be seen that the hybrid material coating covers completely the fabric of polyester. The presence of polypyrrole aggregates that could not be removed from the surface of the fabric was also noticeable. The atomic content of W for this sample was 2.48 %. When it was soaked during 1 h in the pH 1 and pH 7 solutions, the content of W decreased to 2.22 % and 2.17 % respectively (micrographs and analysis not shown). The micrographs did not show any

morphological change. Fig. 6-b shows the EDX analysis and the micrograph for the sample treated at pH 13. The elimination of the counter ion ($PW_{12}O_{40}^{3-}$) from the coating was confirmed since W bands were not observed. Gravimetric measurements showed a significant decrease of the mass of the hybrid material layer; 50 % for the sample treated in basic media due to the loss of the counter ion. Nevertheless, no apparent morphological changes of the polymer layer were observed with higher magnification. The size of this counter ion is approximately 10 Å [55] and its loss could produce a more porous structure. However, SEM magnification was not sufficient to observe this fact. The sample after the washing test was also analyzed by means of EDX (not shown). A decrease of the W content was also noticed (1.66 % atomic), although no changes in the polypyrrole coating were noticed. The data obtained by EDX analysis was consistent with that obtained by XPS measurements and indicated a gradual loss of the counter ion with the increasing pH and a total loss of the counter ion at pH 13.

3.4. Surface resistivity measurements

Surface resistivity measurements were employed to measure variations in the conductivity of the samples due to the different tests performed. In the Fig. 7 the Bode diagrams for different samples of $PES/PPy-PW_{12}O_{40}^{3-}$ are shown. It is shown the data for the original sample of $PES/PPy-PW_{12}O_{40}^{3-}$ and the sample after contact with the different pH solutions (1, 7, 13). The Bode plots for the sample after the washing test are also shown.

In the upper diagram it can be seen the impedance modulus (|Z|) at the different frequencies for the different samples. As it was explained previously, the impedance modulus (Ω) is equivalent to the surface resistivity ($\Omega/\square$) when the material acts as a

resistor; as a square of 1.5 cm was measured. In the text the term impedance modulus is employed but it is equivalent to the surface resistivity. The sample of polyester presents a value of the impedance modulus at low frequencies higher than 10^{11} Ω, typical value of insulating materials. When the sample of polyester was coated with PPy/PW$_{12}$O$_{40}$$^{3-}$, the value of the impedance modulus lowered more than eight orders of magnitude (a value of approximately 250 Ω was obtained). The contact with the pH 1 solution produced a slight increase of the impedance modulus (315 Ω); this drop of the conductivity may be attributed to the loss of part of the counter ion as XPS analysis revealed (50 %). When the sample was treated in the pH 7 solution the impedance modulus rose to 565 Ω. This result is consistent with a decrease of about 65 % in the doping level of PW$_{12}$O$_{40}$$^{3-}$. At pH 13 a large increase of the impedance modulus was observed (9.86·10^5 Ω). The loss of conductivity at pH 13 can be attributed to the deprotonation of polypyrrole that takes place at pH 10 [56] and the reaction of decomposition that PW$_{12}$O$_{40}$$^{3-}$ suffers at pH>8.3 [51]. This loss of conductivity after basic media exposure is consistent with results obtained in bibliography for polypyrrole films [57]. These results corroborate the results obtained by means of XPS and EDX. Nevertheless, the impedance modulus for the sample treated at pH 13 was still lower than that for polyester (5 orders of magnitude for low frequencies). The results for the sample that was submitted to a washing test showed a slight increase of the impedance modulus (698 Ω), slightly higher than the sample treated at pH 7. XPS analysis for the sample after the washing test showed a decrease of about 53 % of the counter ion, this result is consistent with the loss of conductivity observed.

Static charging of the surface of fibers is excluded with surface resistivity below 5·10^9 $\Omega/\square$ [58], so surface resistivity of the conducting textile after the different tests was still

16

adequate for its employment in antistatic applications, including the most adverse conditions that were basic media exposure.

In the second diagram it is shown the data for the phase angle at different frequencies for the same samples of the first diagram. Polyester has a phase angle of nearly 90º, the data at low frequencies is not shown since noise due to the large values of impedance modulus was observed. This value of phase angle is typical of insulating materials that act as a capacitor. All the samples of PES-PPy/PW$_{12}$O$_{40}$$^{3-}$ (except the treated at pH 13) showed values of 0º for the phase angle in the entire frequency range. This indicates that the samples acted as a resistor with the different resistances indicated previously. The sample treated in basic media showed values of phase angle near to 30º at 10^5 Hz, but it decreased to 0º at 10^3 Hz and was 0º in the rest of frequencies (10^3-10^{-2} Hz). Although the treatment in basic media produced a decrease of the conductivity, the sample continued acting as a resistor.

3.5. SECM measurements

SECM was used to measure electroactivity variations of the coatings after the different tests. Approach (I_T–L) curves were recorded in the feedback mode in a 0.01 M solution of Ru(NH$_3$)$_6$$^{3+}$ in 0.1 M KCl, pH ~5.2, using the 100-μm-diameter Pt tip held at a potential of -0.4 V vs Ag/AgCl (3 M KCl). According to the voltammogram in Fig. 8, this potential was selected to reduce the oxidized form of the mediator, Ru(NH$_3$)$_6$$^{3+}$, at a diffusion-controlled rate.

Approach curves give an indication of the electroactivity of the electrode surface. If the surface is non conductive, when the electrode approaches the surface there is a decrease of the current measured (negative feedback) [29]. On the other hand, if the electrode is

conductive, when the electrode approaches the surface of the substrate the current increases (positive feedback) [29].

Figure 9-a, shows a selection of the experimental curves recorded at different points randomly chosen throughout the PES-PPy/PW$_{12}$O$_{40}^{3-}$ treated during 1 h in 0.1 M H$_2$SO$_4$ solution. The line scans show different degrees of positive feedback, ranging among 3.8-4.1. The positive feedback indicates an increase of the normalized current (I) when the microelectrode comes close to the surface, according to its conductive nature; (I = i/i$_\infty$ where i$_\infty$ = 4nFDaC in which n is the number of electrons involved in the reaction, F is the Faraday constant, D is the diffusion coefficient, and a is the radius of the UME). On the other hand, for the sample containing only polyester, negative feedback was obtained (I decreases with the normalized distance L = d/a in which d is the distance between UME and surface). Polyester is an insulating material and negative feedback was obtained (Fig. 9-a, or Fig. 9-b). With this technique it is clearly shown the different electrochemical activity and conductivity of the two surfaces analyzed. Samples soaked in the pH 7 solution showed similar values to the sample soaked in the pH 1 solution, values among 3-4.5 were obtained (figure not shown).

In Fig. 9-b, it is shown the electrochemical activity of PES-PPy/PW$_{12}$O$_{40}^{3-}$ after 1 h of contact with the pH 13 solution. It can be seen a significant decrease of the degree of positive feedback; after the treatment with the pH 13 solution the values obtained were among 0.9-1.4. There has been a decrease of the material electroactivity due to the deprotonation of polypyrrole that takes place at pH 10 [56] and the elimination of the counter ion from the coating. However, the conducting fabric continued showing some degree of positive feedback, it can be appreciated the difference with the results for the

PES sample. These results are consistent with EIS measurements that showed a loss of its conducting properties, but the material continued acting as a conductor.

4. Conclusions

Conductive fabrics of PES-PPy/$PW_{12}O_{40}^{3-}$ are stable in acid media and neutral media. As pH increases, there is an expulsion of part of the counter ions from the polymer matrix. The direct effect was the increase in the surface resistivity of the conducting fabric. The increase of the surface resistivity in acid and neutral media was small, as well as after the washing test. On the other hand, in basic medium a large increase of the surface resistivity was observed, more than three orders. At pHs>8.4, the decomposition reaction of the counter ion is another factor that influences the loss of conductivity. The different tests produced a loss of conductivity but its conducting nature was not modified; the samples continued acting mainly as a resistor, without capacitative behavior. The sample treated in basic medium merits special mention because it continued acting as a resistor (except at high frequencies) regardless the noticeable loss of conductivity. The surface resistivity of the conducting textile after the different tests was still adequate (below $5 \cdot 10^9$ $\Omega/\square$) for its employment in antistatic applications.

SECM measurements showed that the coatings of PPy/$PW_{12}O_{40}^{3-}$ were electroactive after the tests in acid and neutral media. The treatment in the pH 13 solution caused a significant decrease of its electroactivity, this decrease is related to the deprotonation of polypyrrole and the loss of the counter ion from the polymer matrix. Zonal EDX analyses showed similar results to that obtained by XPS measurements. SEM micrographs did not show morphological changes in the fibers surface. The loss of the

counter ion would produce a more porous structure, however the small size of the counter ion (10 Å approximately) and SEM resolution was not sufficient to observe this effect.

References

[1] P. Lekpittaya, N. Yanumet, B.P. Grady, E.A. O'Rear, Resistivity of conductive polymer-coated fabric, J. Appl. Polym. Sci. 92 (2004) 2629-2636.

[2] D. Kincal, A. Kumar, A. Child, J. Reynolds, Conductivity switching in polypyrrole-coated textile fabrics as gas sensors, Synth. Met. 92 (1998) 53-56.

[3] J. Wu, D. Zhou, C.O. Too, G.G. Wallace, Conducting polymer coated lycra, Synth. Met. 155 (2005) 698-701.

[4] K.W. Oh, H.J. Park, S.H. Kim, Stretchable conductive fabric for electrotherapy, J. Appl. Polym. Sci. 88 (2003) 1225-1229.

[5] S.H. Kim, K.W. Oh, J.H. Bahk, Electrochemically synthesized polypyrrole and Cu-plated nylon/spandex for electrotherapeutic pad electrode, J. Appl. Polym. Sci. 91 (2004) 4064-4071.

[6] N.V. Bhat, D.T. Seshadri, M.N. Nate, A.V. Gore, Development of conductive cotton fabrics for heating devices, J. Appl. Polym. Sci. 102 (2006) 4690-4695.

[7] E. Hakansson, A. Kaynak, T. Lin, S. Nahavandi, T. Jones, E. Hu, Characterization of conducting polymer coated synthetic fabrics for heat generation, Synth. Met. 144 (2004) 21-28.

[8] J.P. Boutrois, R. Jolly, C. Pétrescu, Process of polypyrrole deposit on textile. Product characteristics and applications, Synth. Met. 85 (1997) 1405-1406.

[9] H. Kuhn, A. Child, W. Kimbrell, Toward real applications of conductive polymers, Synth. Met. 71 (1995) 2139-2142.

[10] K.G. Neoh, T.T. Young, E.T. Kang, K.L. Tan, Structural and mechanical degradation of polypyrrole films due to aqueous media and heat treatment and the subsequent redoping characteristics, J. Appl. Polym. Sci. 64 (1997) 519-526.

[11] T. Lin, L. Wang, X. Wang, A. Kaynak, Polymerising pyrrole on polyester textiles and controlling the conductivity through coating thickness, Thin Solid Films 479 (2005) 77-82.

[12] F. Ferrero, L. Napoli, C. Tonin, A. Varesano, Pyrrole chemical polymerization on textiles: Kinetics and operating conditions, J. Appl. Polym. Sci. 102 (2006) 4121-4126.

[13] S. Garg, C. Hurren, A. Kaynak, Improvement of adhesion of conductive polypyrrole coating on wool and polyester fabrics using atmospheric plasma treatment, Synth. Met. 157 (2007) 41-47.

[14] J. Molina, A.I. del Río, J. Bonastre, F. Cases, Chemical and electrochemical polymerisation of pyrrole on polyester textiles in presence of phosphotungstic acid. Eur. Poly. J. 44 (2008) 2087-2098.

[15] H.S. Lee, J. Hong, Chemical synthesis and characterization of polypyrrole coated on porous membranes and its electrochemical stability, Synth. Met. 113 (2000) 115-119.

[16] E. Gasana, P. Westbroek, J. Hakuzimana, K. De Clerck, G. Priniotakis, P. Kiekens, D. Tseles, Electroconductive textile structures through electroless deposition of polypyrrole and copper at polyaramide surfaces, Surf. Coat. Technol. 201 (2006) 3547-3551.

[17] L. Dall'Acqua, C. Tonin, A. Varesano, M. Canetti, W. Porzio, M. Catellani, Vapour phase polymerisation of pyrrole on cellulose-based textile substrates, Synth. Met. 156 (2006) 379-386.

[18] L. Dall'Acqua, C. Tonin, R. Peila, F. Ferrero, M. Catellani, Performances and properties of intrinsic conductive cellulose–polypyrrole textiles, Synth. Met. 146 (2004) 213-221.

[19] P. Gómez-Romero, Hybrid Organic-Inorganic Materials - In Search of Synergic Activity, Adv. Mater. 13 (2001) 163-174.

[20] P. Kormali, T. Triantis, D. Dimotikali, A. Hiskia, E. Papaconstantinou, On the photooxidative behavior of TiO_2 and $PW_{12}O_{40}^{3-}$: OH radicals versus holes, Appl. Catal. B-Environ. 68 (2006) 139-146.

[21] B.M. Devassy, F. Lefebvre, S.B. Halligudi, Zirconia-supported 12-tungstophosphoric acid as a solid catalyst for the synthesis of linear alkyl benzenes, J. Catal. 231 (2005) 1-10.

[22] K. Bouzek, K.-M. Mangold, K. Jüttner, Electrocatalytic activity of platinum modified polypyrrole films for the methanol oxidation reaction, J. Appl. Electrochem. 31 (2001) 501-507.

[23] L. Li, Y. Zhang, J.-F. Drillet, R. Dittmeyer, K.-M. Jüttner, Preparation and characterization of Pt direct deposition on polypyrrole modified Nafion composite membranes for direct methanol fuel cell applications, Chem. Eng. J. 133 (2007) 113-119.

[24] F.J. Rodríguez, S. Gutiérrez, J.S. Ibanez, J.L. Bravo, N. Batina, The efficiency of toxic chromate reduction by a conducting polymer (polypyrrole): influence of electropolymerization conditions, Environ. Sci. Technol. 34 (2000) 2018-2023.

[25] Y. Tian, J. Wang, Z. Wang, S. Wang, Electroreduction of nitrite at an electrode modified with polypyrrole nanowires, Synth. Met. 143 (2004) 309-313.

[26] A. Lopes, S. Martins, A. Moraö, M. Magrinho, I. Gonçalves, Degradation of a textile dye C. I. Direct Red 80 by electrochemical processes, Port. Electrochim. Acta 22 (2004) 279-294.

[27] A.H. Gemeay, R.G. El-Sharkawy, I.A. Mansour, A.B. Zaki, Catalytic activity of polyaniline/MnO_2 composites towards the oxidative decolorization of organic dyes, Appl. Catal. B-Environ. 80 (2008) 106-115.

[28] A.H. Gemeay, R.G. El-Sharkawy, I.A. Mansour, A.B. Zaki, Preparation and characterization of polyaniline/manganese dioxide composites and their catalytic activity, J. Colloid Interf. Sci. 308 (2007) 385-394.

[29] P. Sun, F.O. Laforge, M.V. Mirkin, Scanning electrochemical microscopy in the 21st century, Phys. Chem. Chem. Phys. 9 (2007) 802-823.

[30] M.V. Mirkin, B.R. Horrocks, Electroanalytical measurements using the scanning electrochemical microscope, Anal. Chim. Acta 406 (2000) 119-146.

[31] A.L. Barker, M. Gonsalves, J.V. Macpherson, C.J. Slevin, P.R. Unwin, Scanning electrochemical microscopy: beyond the solid/liquid interface, Anal. Chim. Acta 385 (1999) 223-240.

[32] Complete textile glossary, Available from: http://www.celaneseacetate.com/textile_glossary_filament_acetate.pdf, 2001. Last accessed 17th May 2010.

[33] J.M. Ribo, A. Dicko, J.M. Tura, D. Bloor, Chemical structure of polypyrrole: X-ray photoelectron spectroscopy of polypyrrole with 5-yliden-3-pyrrolin-2-one end groups, Polymer 32 (1991) 728-732.

[34] J.C. Thiéblemont, J.L. Gabelle, M.F. Planche, Polypyrrole overoxidation during its chemical synthesis, Synth. Met. 66 (1994) 243-247.

[35] R. Rajagopalan, J.O. Iroh, Characterization of polyaniline-polypyrrole composite coatings on low carbon steel: a XPS and infrared spectroscopy study, Appl. Surf. Sci. 218 (2003) 58-69.

[36] W. Prissanaroon-Ouajai, P.J. Pigram, R. Jones, A. Sirivat, A novel pH sensor based on hydroquinone monosulfonate-doped conducting polypyrrole, Sensor. Actuat. B-Chem. 135 (2008) 366-374.

[37] L.G. Paterno, S. Manolache, F. Denes, Synthesis of polyaniline-type thin layer structures under low-pressure RF-plasma conditions, Synth. Met. 130 (2002) 85-97.

[38] L. Sabbatini, C. Malitesta, E. De Giglio, I. Losito, L. Torsi, P.G. Zambonin, Electrosynthesised thin polymer films: the role of XPS in the design of application oriented innovative materials, J. Electron. Spectrosc. Relat. Phenom. 100 (1999) 35-53.

[39] J. Starck, P. Burg, S. Muller, J. Bimer, G. Furdin, P. Fioux, C.V. Guterl, D. Begin, P. Faure, B. Azambre, The influence of demineralisation and ammoxidation on the adsorption properties of an activated carbon prepared from a Polish lignite, Carbon 44 (2006) 2549-2557.

[40] C.G.J. Koopal, M.C. Feiters, R.J.M. Nolte, B. de Ruiter, R.B.M. Schasfoort, R. Czajka, H. Van Kempen, Polypyrrole microtubules and their use in the construction of a third generation biosensor, Synth. Met. 51 (1992) 397-405.

[41] L. Pesaresi, D.R. Brown, A.F. Lee, J.M. Montero, H. Williams, K. Wilson, Cs-doped $H_4SiW_{12}O_{40}$ catalysts for biodiesel applications, Appl. Catal. A-Gen. 360 (2009) 50-58.

[42] M. Wahlqvist, A. Shchukarev, XPS spectra and electronic structure of Group IA sulfates, J. Electron. Spectrosc. Relat. Phenom. 156–158 (2007) 310-314.

[43] S. Carquigny, O. Segut, B. Lakard, F. Lallemand, P. Fievet, Effect of electrolyte solvent on the morphology of polypyrrole films: Application to the use of polypyrrole in pH sensors, Synth. Met. 158 (2008) 453-461.

[44] J. Mansouri, R.P. Burford, Characterization of PVDF-PPy composite membranes, Polymer 38 (1997) 6055-6069.

[45] L.E. Briand, H.J. Thomas, G.T. Baronetti, Thermal stability and catalytic activity of Wells-Dawson tungsten heteropoly salts, Appl. Catal. A-Gen. 201 (2000) 191-202.

[46] P.A. Jalil, M. Faiz, N. Tabet, N.M. Hamdan, Z. Hussain, A study of the stability of tungstophosphoric acid, $H_3PW_{12}O_{40}$, using synchrotron XPS, XANES, hexane cracking, XRD, and IR spectroscopy, J. Catal. 217 (2003) 292-297.

[47] Q. Liu, P. Jia, H. Chen, Study on catalytic membranes of $H_3PW_{12}O_{40}$ entrapped in PVA, J. Membrane Sci. 159 (1999) 233-241.

[48] L. Zhang, Y.H. Shen, A.J. Xie, S.K. Lia, C. Wang, One-step synthesis of silver nanoparticles in self-assembled multilayered films based on a Keggin structure compound, J. Mater. Chem. 18 (2008) 1196-1203.

[49] B. Dong, J. Peng, P. Zhang, A. Tian, J. Chen, B. Xue, Hydrothermal synthesis and crystal structure of a novel Keggin polyoxoanion-templated multichain coordination polymer with a flexible bis(imidazole) ligand, Inorg. Chem. Commun. 10 (2007) 839-842.

[50] C.D. Wagner, A.V. Naumkin, A. Kraut-Vass, J.W. Allison, C.J. Powell, J.R. Rumble Jr., X-Ray Photoelectron Spectroscopy Database, The National Institute of Standards and Technology, U.S. Secretary of Commerce, Available from: http://srdata.nist.gov/xps, 2007. Last accessed 17th May 2010.

[51] Z. Zu, R. Tain, C. Rhodes, A study of the decomposition behaviour of 12-tungstophosphate heteropolyacid in solution, Can. J. Chem. 81 (2003) 1044-1050.

[52] S. Aeiyach, B. Zaid, P.C. Lacaze, A one-step electrosynthesis of PPy films on zinc substrates by anodic polymerization of pyrrole in aqueous solution, Electrochim. Acta 44 (1999) 2889-2898.

[53] C. Hurren, A. Kaynak, X. Wang, Effects of laundering on conductivity of polypyrrole-coated textiles, Res. J. Text. Appar. 11 (2007) 11-17.

[54] A. Varesano, L. Dall'Acqua, C. Tonin, A study on the electrical conductivity decay of polypyrrole coated wool textiles, Polym. Degrad. Stabil. 89 (2005) 125-132.

[55] E. López-Salinas, J.G. Hernández-Cortéz, M.A. Cortés-Jácome, J. Navarrete, M.E. Llanos, A. Vázquez, H. Armendáriz, T. López, Skeletal isomerization of 1-butene on 12-tungstophosphoric acid supported on zirconia, Appl. Catal. A-Gen. 175 (1998) 43-53.

[56] M. Krzysztof, Chemical reactivity of polypyrrole and its relevance to polypyrrole based electrochemical sensors, Electroanal. 18 (2006) 1537-1551.

[57] Y. Li, J. Ouyang, J. Yang, Two doping structures and structural anisotropy revealed by the mass loss and shrinkage of polypyrrole films on alkali treatment, Synth. Met. 74 (1995) 49-53.

[58] T. Textor, B. Mahltig, A sol–gel based surface treatment for preparation of water repellent antistatic textiles, Appl. Surf. Sci. 256 (2010) 1668–1674.

Figure captions

Fig. 1. C1s XPS core level spectrum for untreated PPy/POM sample.

Fig. 2. O1s XPS core level spectrum for untreated PPy/POM sample.

Fig. 3. N1s XPS core level spectrum for untreated PPy/POM sample.

Fig. 4. N1s XPS core level spectrum for PPy/POM sample treated at pH 13.

Fig. 5. W4f XPS core level spectrum for untreated PPy/POM sample.

Fig. 6. Micrographs and EDX measurements of PES-PPy/$PW_{12}O_{40}{}^{3-}$ (a) and PES-PPy/$PW_{12}O_{40}{}^{3-}$ + 1h pH 13 (b).

Fig. 7. Bode plots for PES, PES+PPy/$PW_{12}O_{40}^{3-}$ chemically synthesized, treated during 1 h with pH 1, pH 7 and pH 13 and after the washing test. Measurements between two copper electrodes above the samples. Distance between electrodes 1.5 cm. Textile measured area 1.5 cm x 1.5 cm. Frequency range from 10^5 Hz to 10^{-2} Hz.

Fig. 8. Cyclic voltammograms for Pt UME 100-µm-diameter tip. The UME potential was scanned from +100 to -700 mV (vs Ag/AgCl) in a 0.01 M $Ru(NH_3)_6^{3+}$ and 0.1 M KCl at 50 mV s^{-1}.

Fig. 9. Approaching curves for: a) PES (---), PES-PPy/AQSA + 1 h pH 1 (—) and b) PES-PPy/AQSA + 1 h pH 13 (—); obtained with a 100 µm diameter Pt tip in 0.01 M $Ru(NH_3)_6^{3+}$ and 0.1 M KCl. The tip potential was -400 mV (vs Ag/AgCl) and the approach rate was 10 µm s^{-1}.

Table captions

Table 1. XPS surface compositional data for the selected samples.

Table 2. XPS assignments for binding energies (eV) of different conducting textiles.
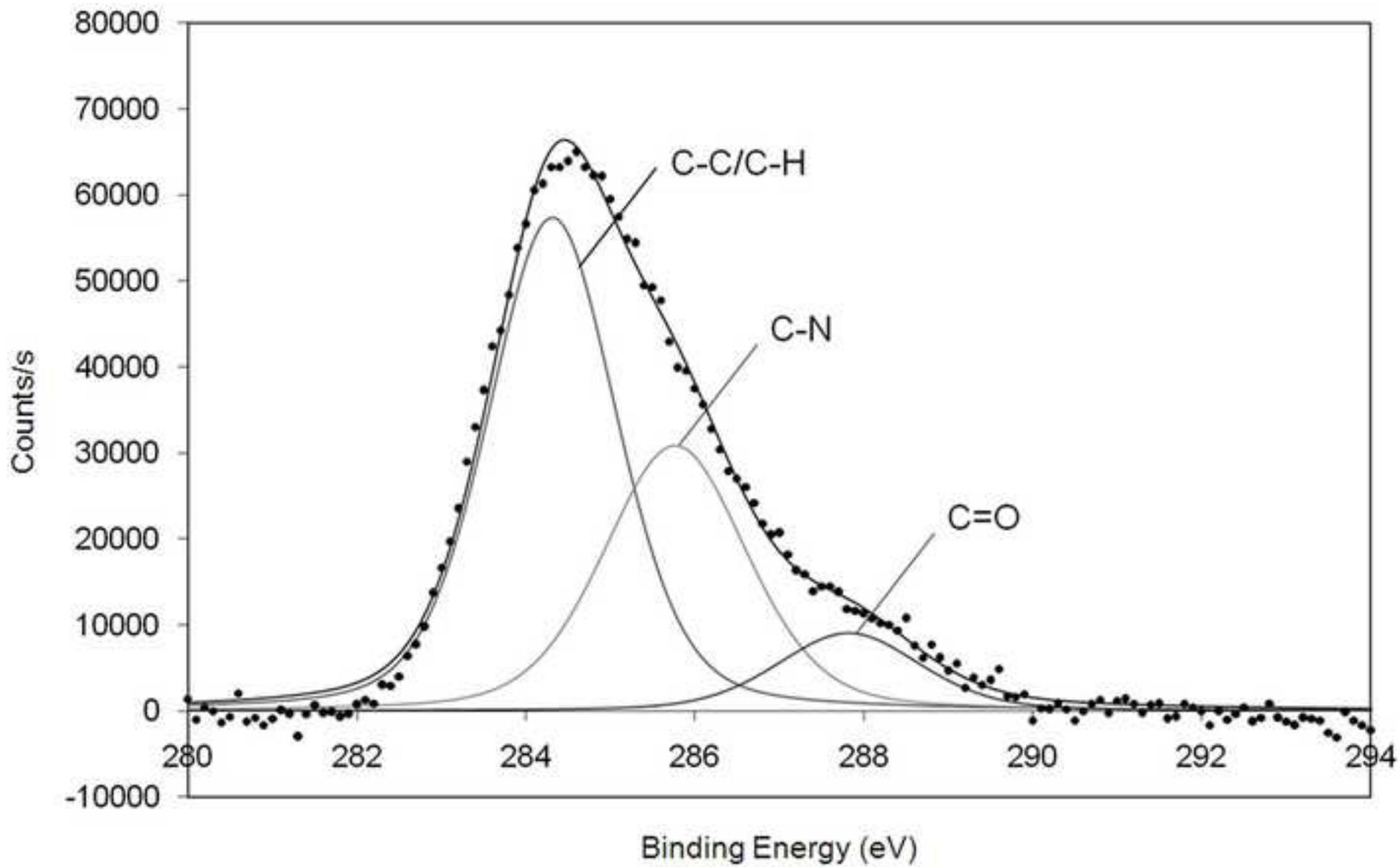
Figure(2)
Click here to download high resolution image
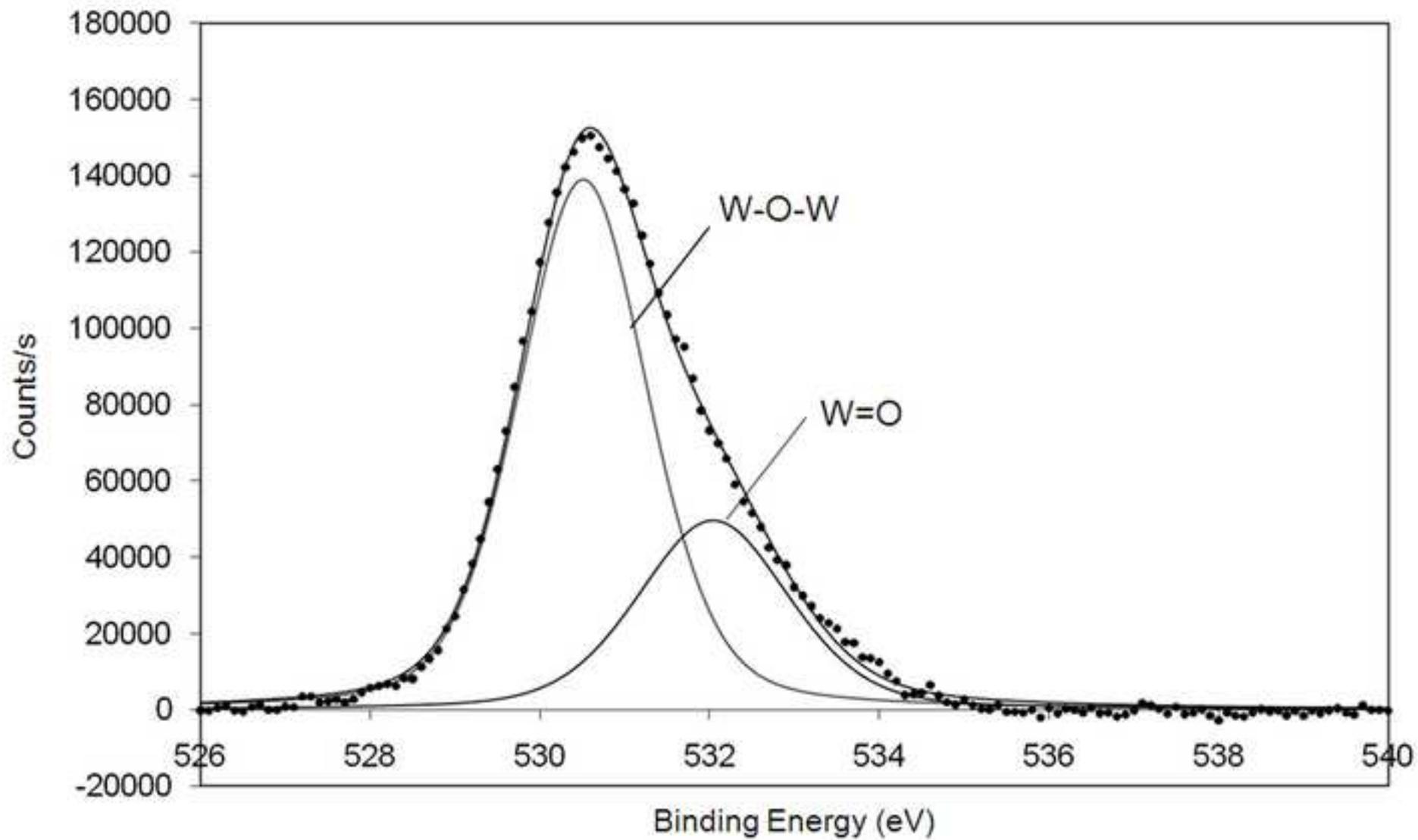
Figure(3)
Click here to download high resolution image
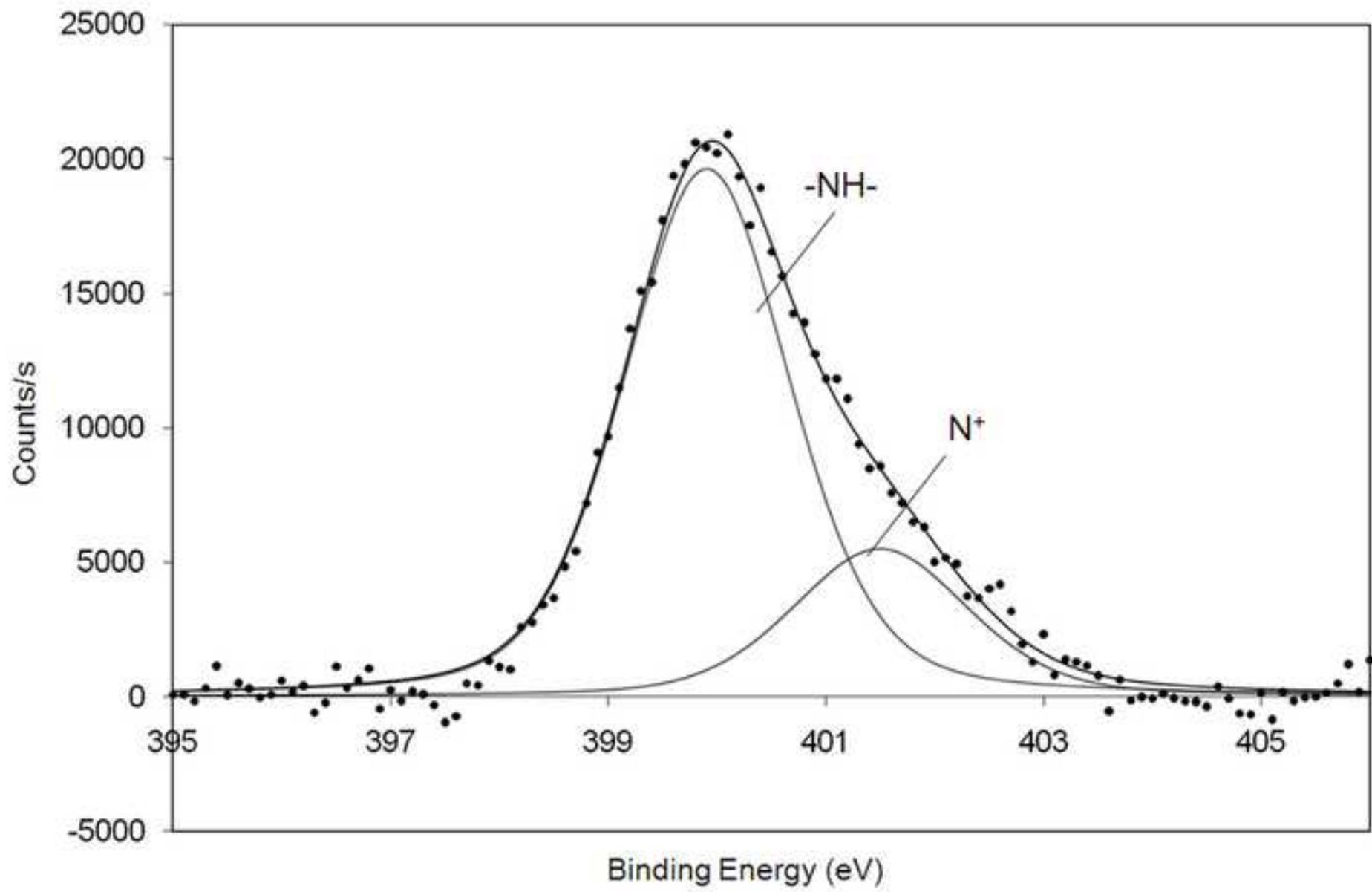
Figure(4)
**Click here to download high resolution image**
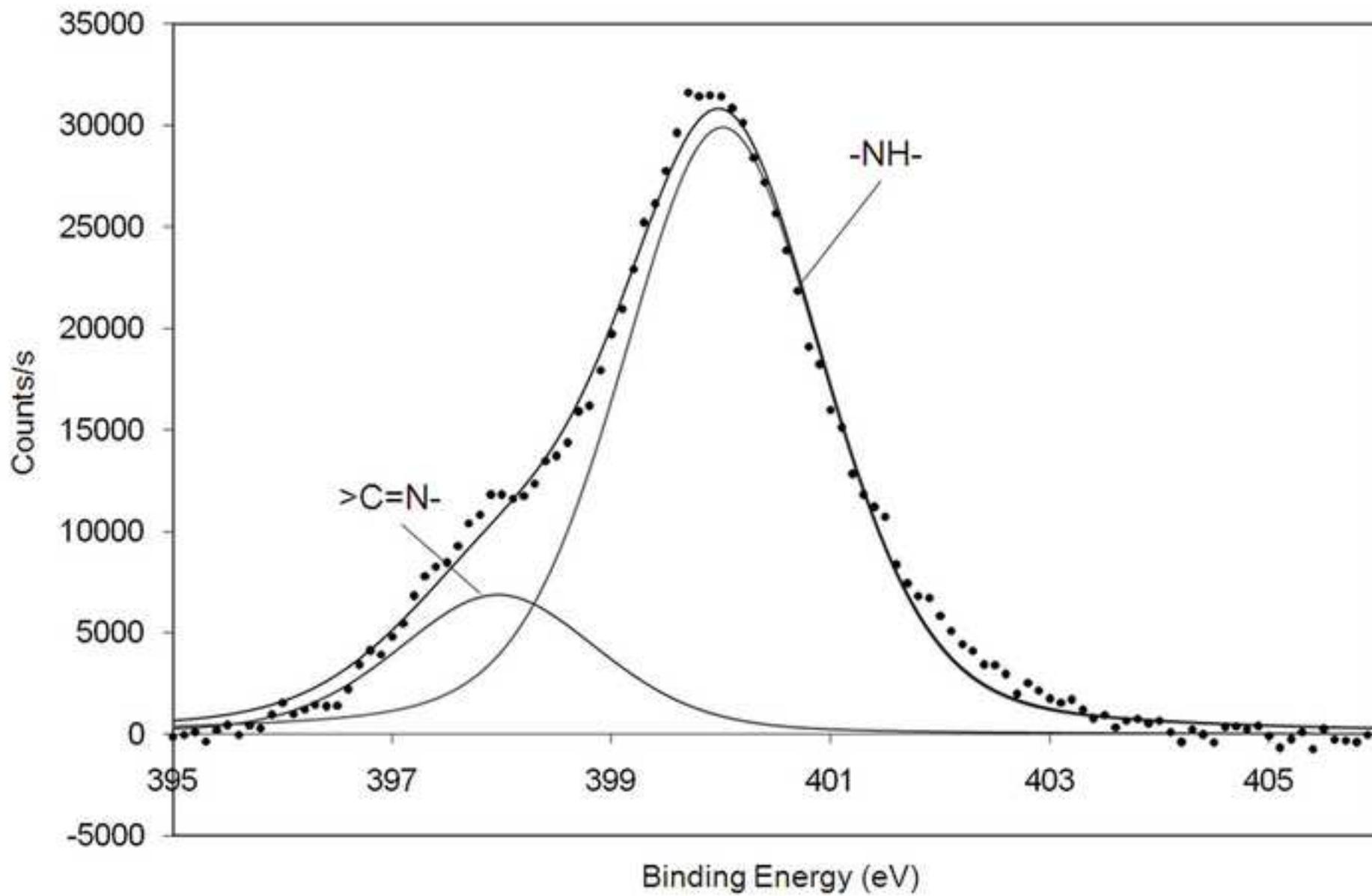
a)
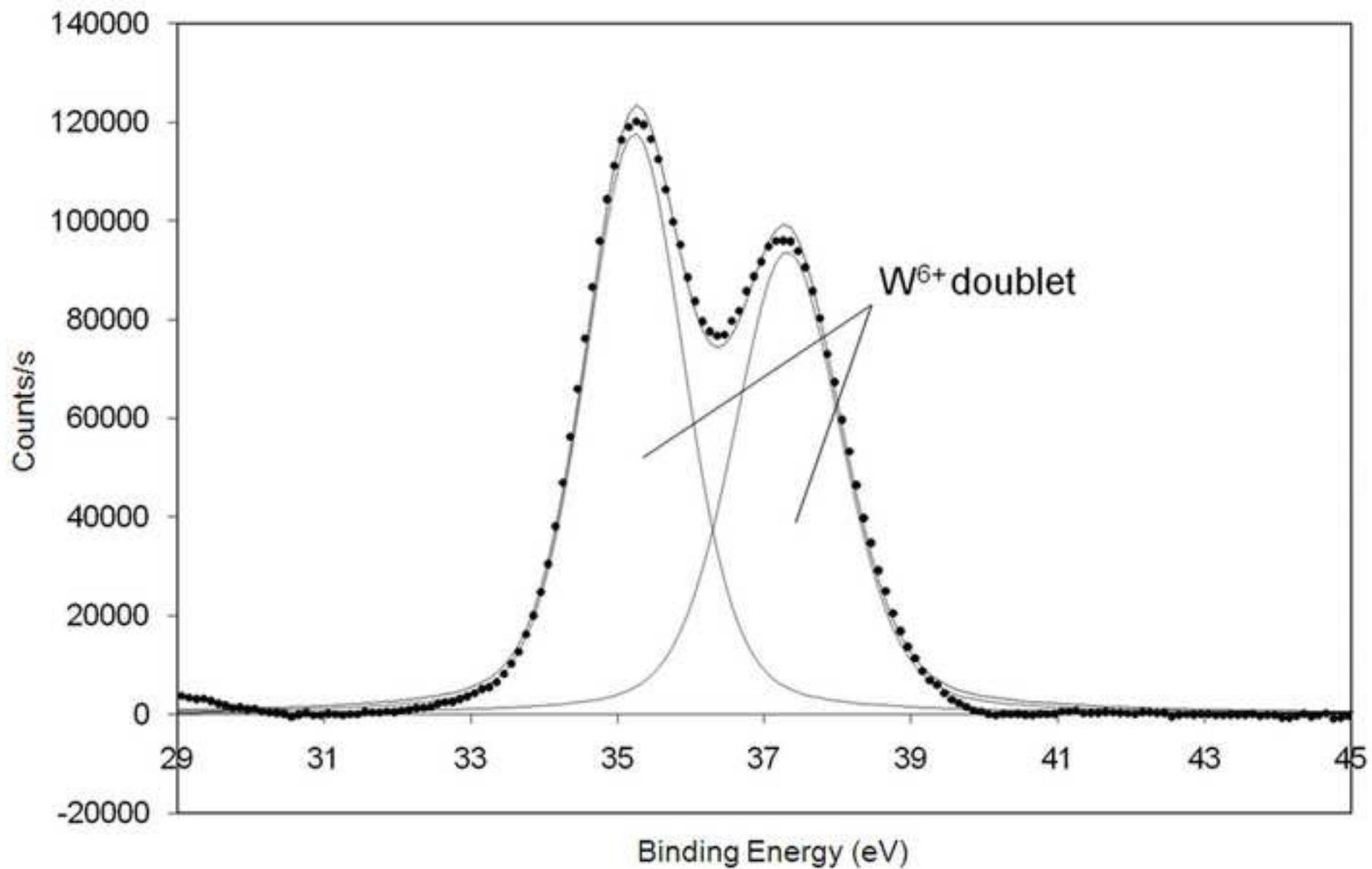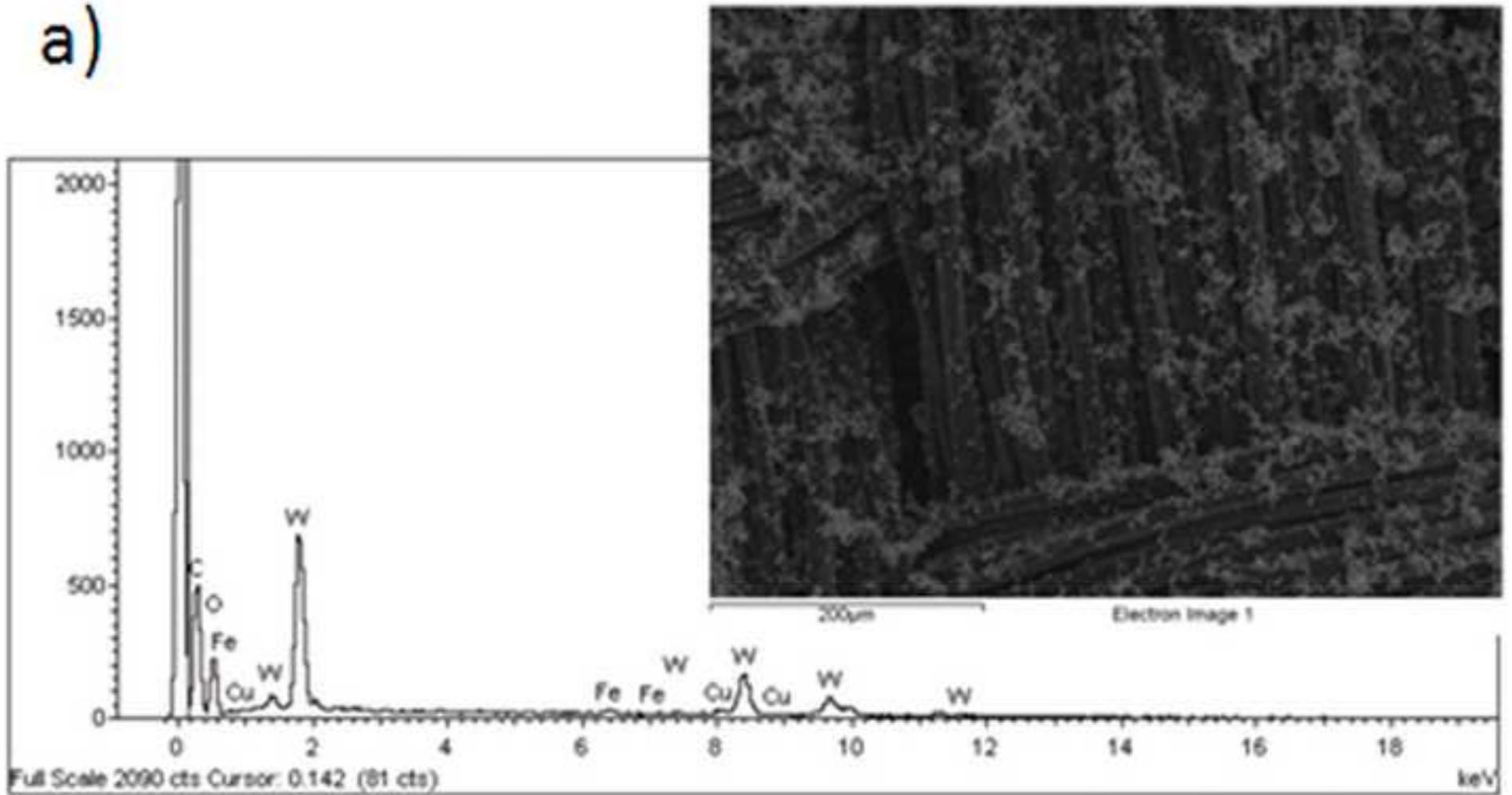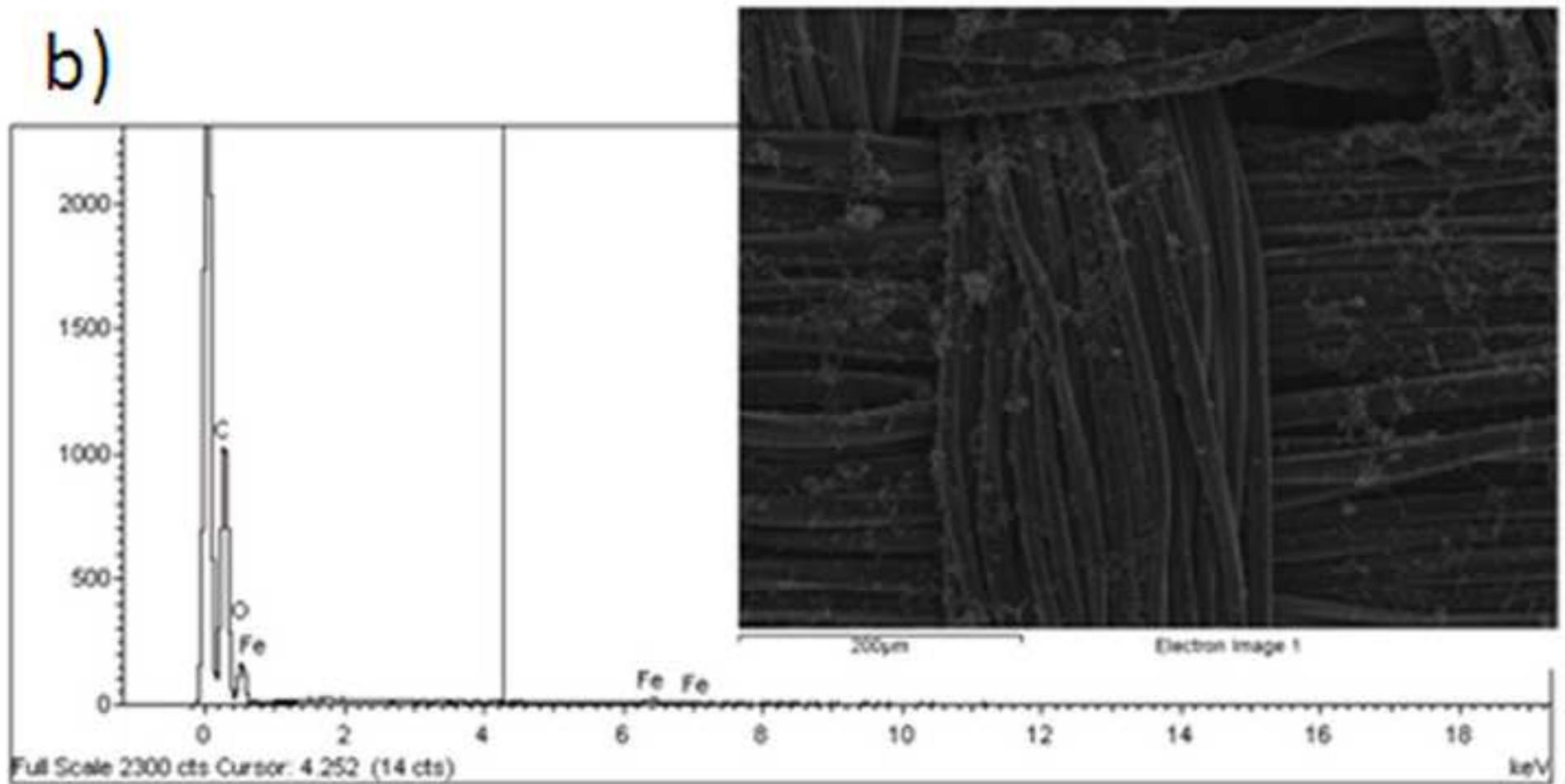
Figure(7)
Click here to download high resolution image
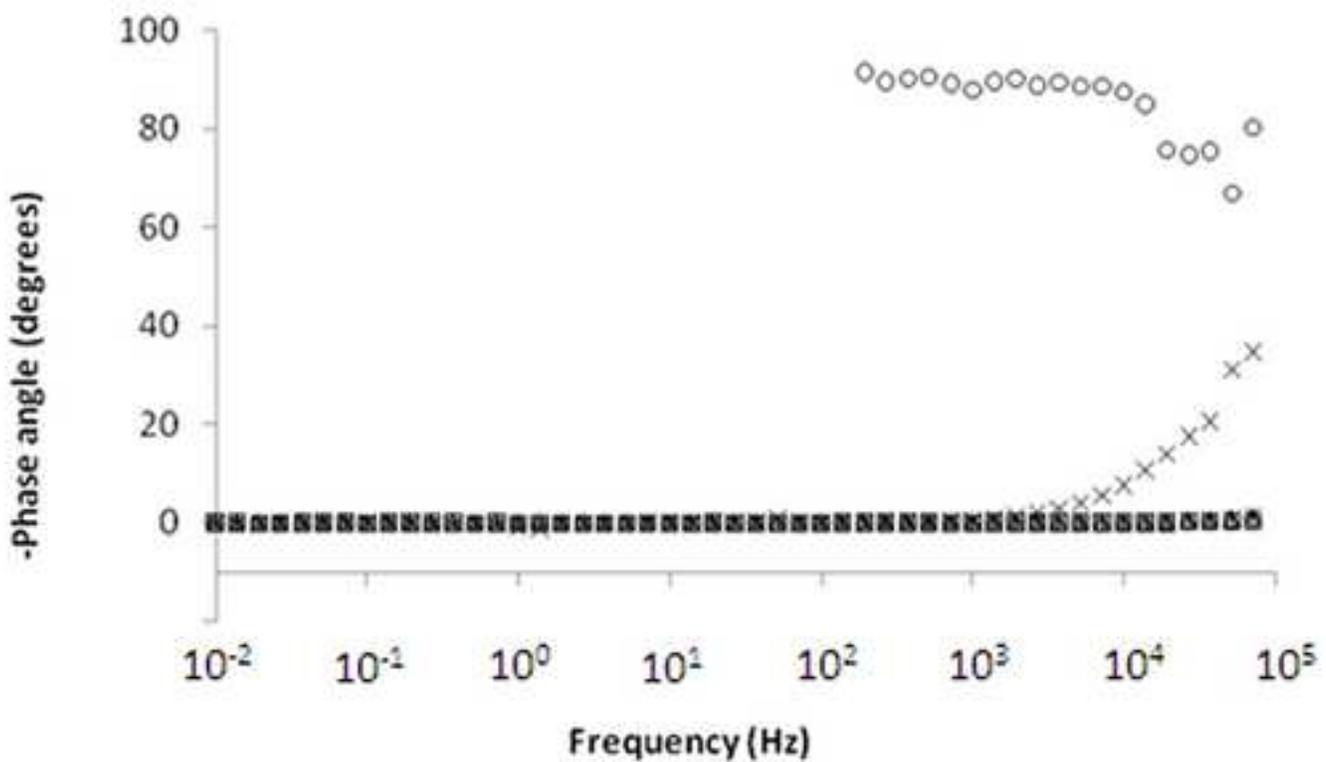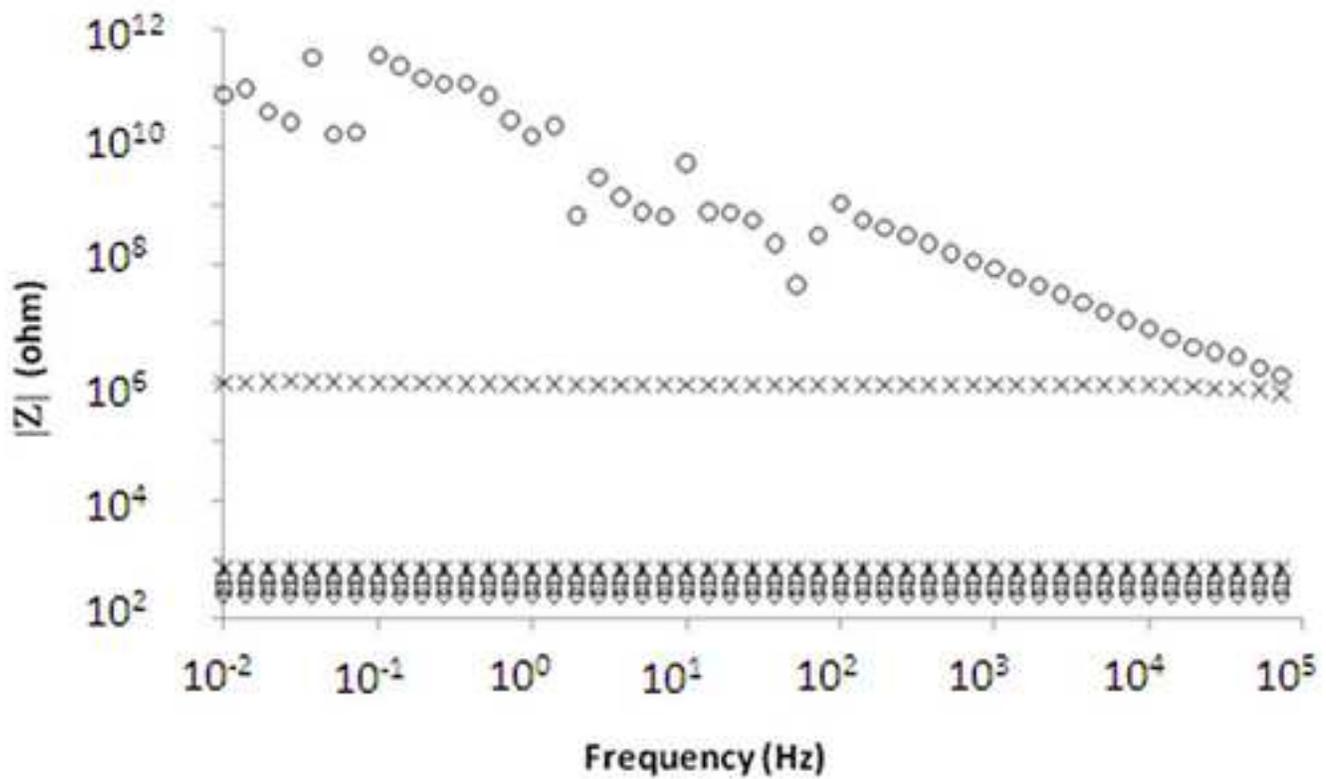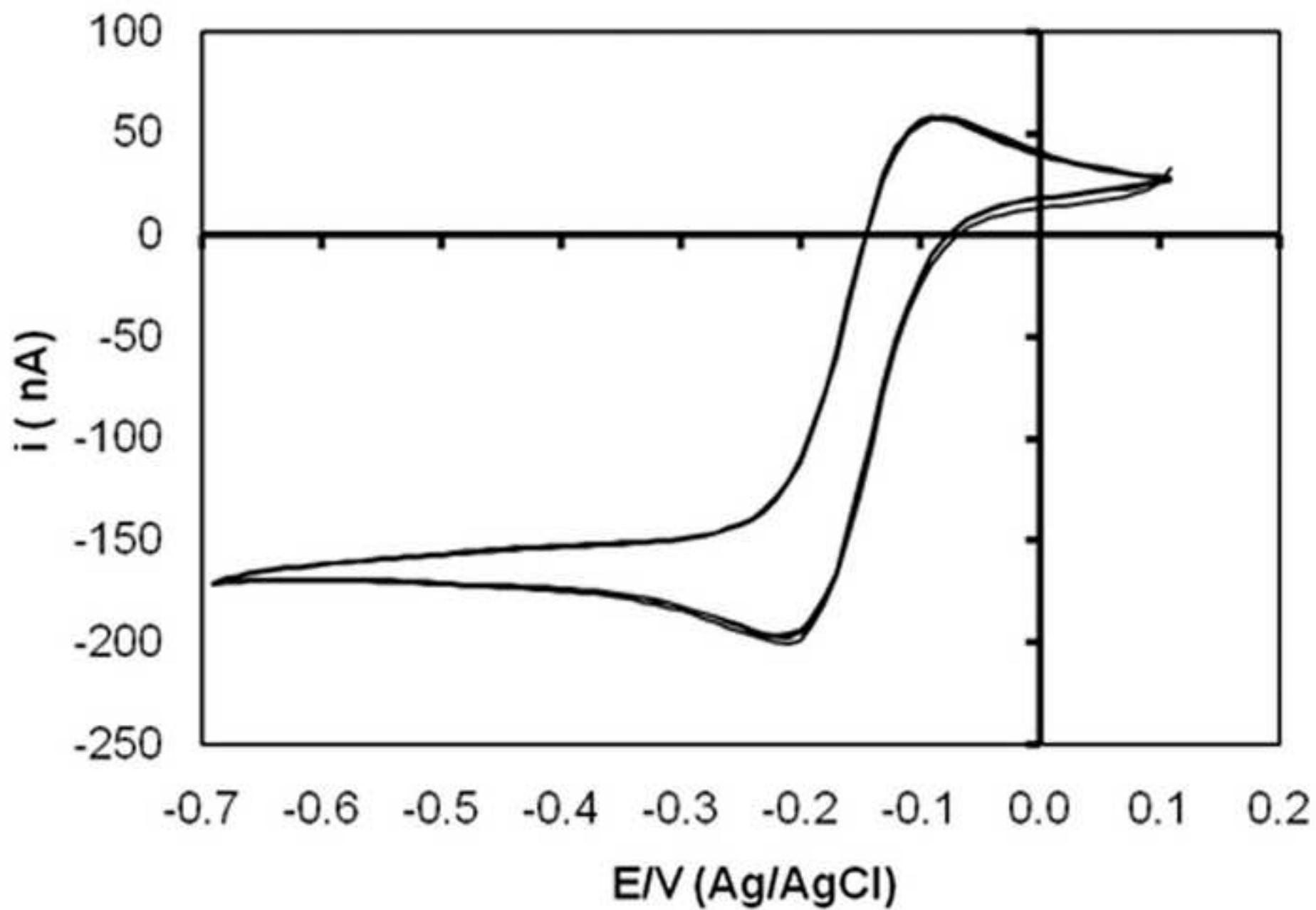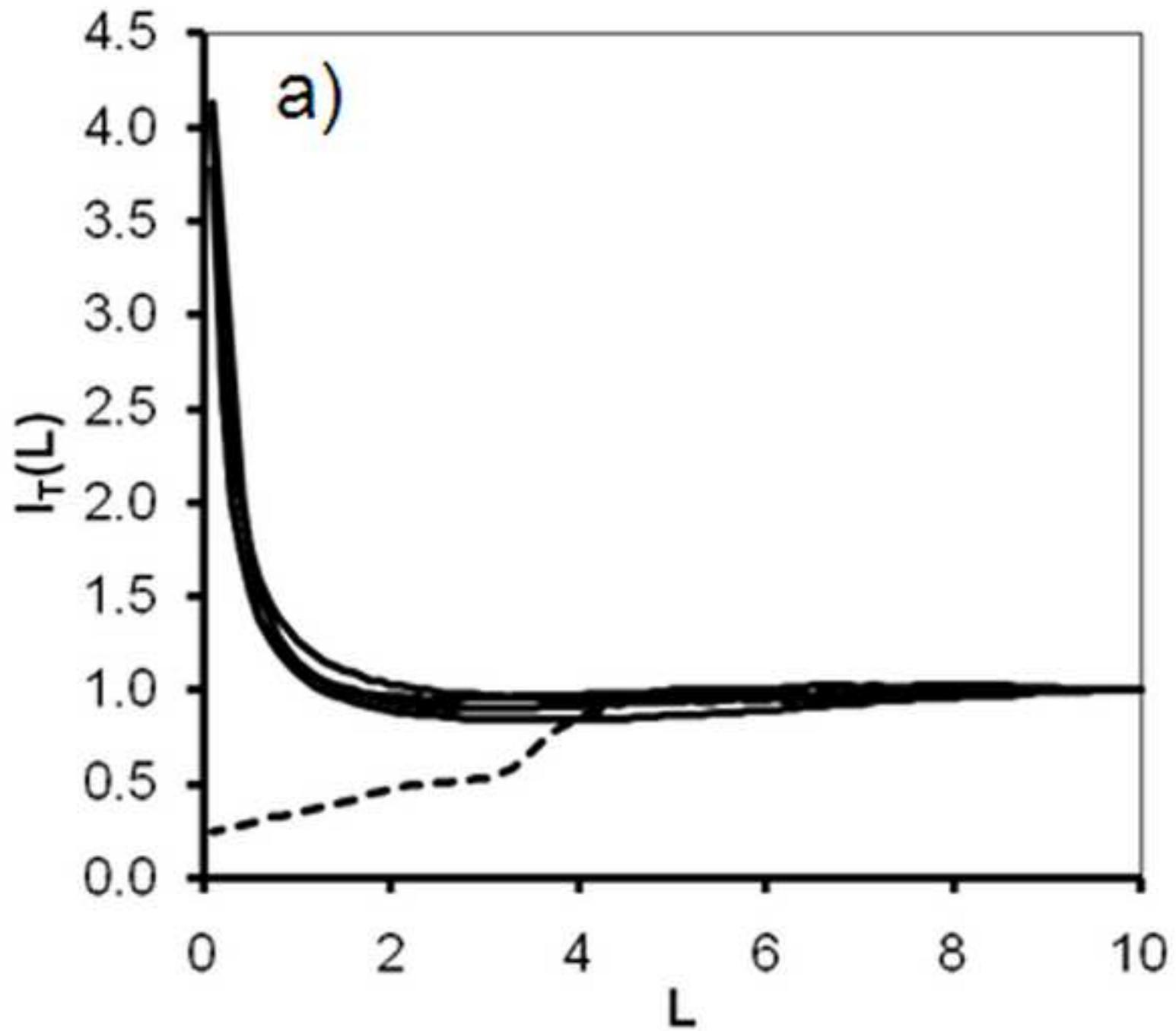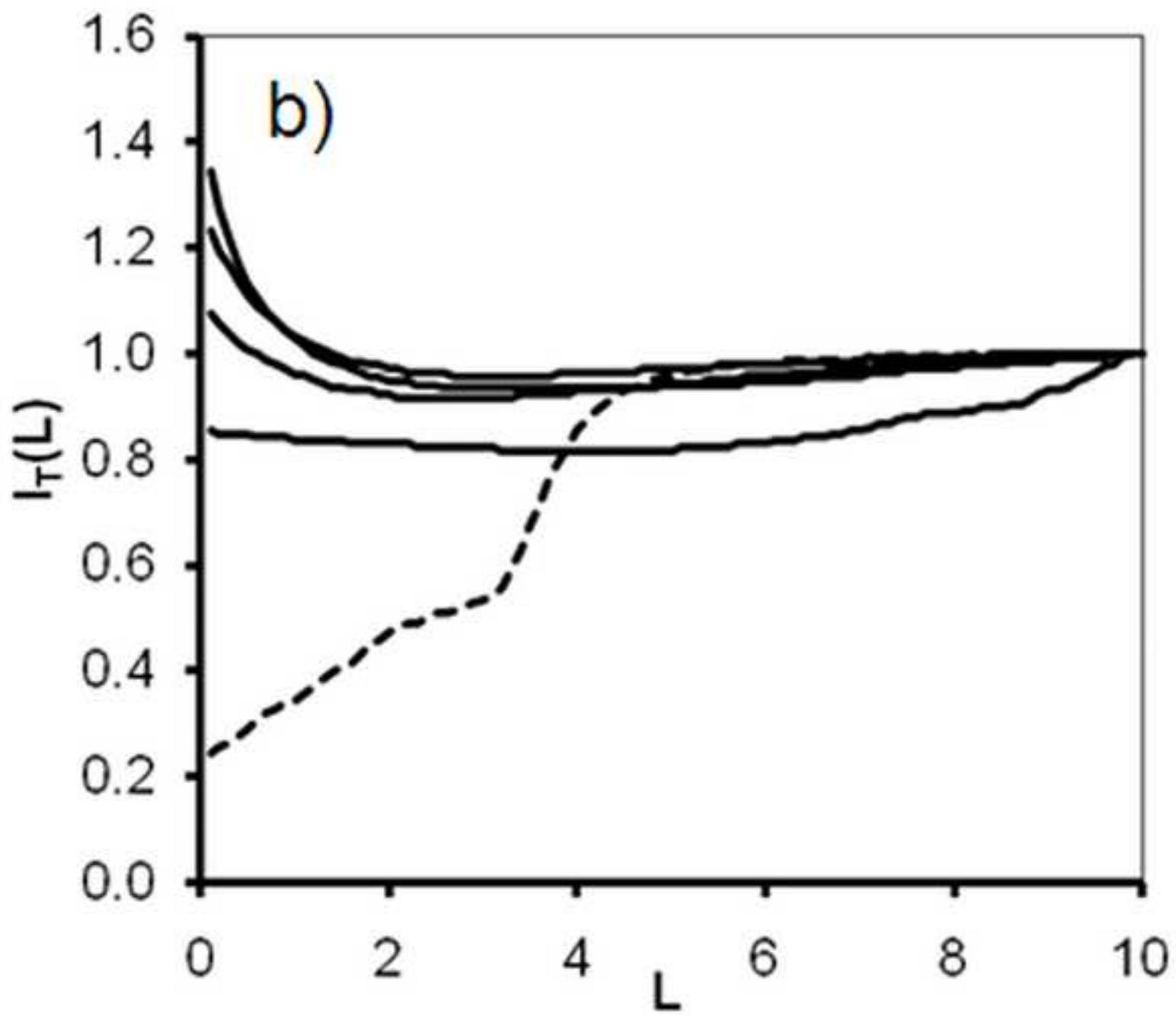
Table(1)
**Click here to download high resolution image**

Sample code	Sample	Chemical composition	Doping ratio (N^+/N)
1	PPy/POM	$C_{6.75}N(PW_{12}O_{40}^{3-})_{0.115}O_{0.32}$	0.23
2	PPy/POM treated at pH 1	$C_{4.90}N(PW_{12}O_{40}^{3-})_{0.057}(SO_4^{2-})_{0.057}O_{0.25}$	0.20
3	PPy/POM treated at pH 7	$C_{5.89}N(PW_{12}O_{40}^{3-})_{0.04}(SO_4^{2-})_{0.057}O_{066}$	0.27
4	PPy/POM treated at pH 13	$C_{5.73}N(PW_{12}O_{40}^{3-})_{0.0008}(SO_4^{2-})_{0.025}O_{1.04}$	0.00

Table(2)

	PPy/POM Sample 1	PPy/POM Sample 2 (pH 1)	PPy/POM Sample 2 (pH 7)	PPy/POM Sample 3 (pH 13)	Assignments
	284.3	284.2	284.3	284.5	C-C/C-H
C1s	285.8	285.5	285.6	285.7	C-N
	287.8	287.6	287.8	287.7	C=O
	530.5	530.5	530.6	-	W-O-W
	532.0	532.2	532.2	-	W=O
O1s	-	-	-	530.5	C=O
	-	-	-	531.9	SO_4^{2-}
	-	-	-	533.6	C=O-C
	-	-	-	398.0	>C=N-
N1s	399.9	399.9	399.8	400.0	NH
	401.5	401.4	401.0	-	N+
W4f	35.4	35.3	35.3	35.2	W^{6+} (4f7/2)
	37.5	37.4	37.4	37.3	W^{6+} (4f5/2)
S2p	-	168.2	168.2	168.4	SO_4^{2-} (S2p3/2)
	-	169.6	169.7	169.7	SO_4^{2-} (S2p1/2)
P2p	133.7	133.9	133.7	-	P^{5+}